Bacterial flagella explore microscale hummocks and hollows to increase adhesion

Ronn S. Friedlander[a,b], Hera Vlamakis[c], Philseok Kim[b,d], Mughees Khan[b], Roberto Kolter[c], and Joanna Aizenberg[b,d,e,1]

[a]Harvard–Massachusetts Institute of Technology Division of Health Sciences and Technology, Cambridge, MA 02139; [c]Department of Microbiology and Immunobiology, Harvard Medical School, Boston, MA 02115; and [d]School of Engineering and Applied Sciences, [b]Wyss Institute for Biologically Inspired Engineering, and [e]Kavli Institute for Bionano Science and Technology, Harvard University, Cambridge, MA 02138

Edited by Pablo Gaston Debenedetti, Princeton University, Princeton, NJ, and approved February 23, 2013 (received for review November 14, 2012)

Biofilms, surface-bound communities of microbes, are economically and medically important due to their pathogenic and obstructive properties. Among the numerous strategies to prevent bacterial adhesion and subsequent biofilm formation, surface topography was recently proposed as a highly nonspecific method that does not rely on small-molecule antibacterial compounds, which promote resistance. Here, we provide a detailed investigation of how the introduction of submicrometer crevices to a surface affects attachment of *Escherichia coli*. These crevices reduce substrate surface area available to the cell body but increase overall surface area. We have found that, during the first 2 h, adhesion to topographic surfaces is significantly reduced compared with flat controls, but this behavior abruptly reverses to significantly increased adhesion at longer exposures. We show that this reversal coincides with bacterially induced wetting transitions and that flagellar filaments aid in adhesion to these wetted topographic surfaces. We demonstrate that flagella are able to reach into crevices, access additional surface area, and produce a dense, fibrous network. Mutants lacking flagella show comparatively reduced adhesion. By varying substrate crevice sizes, we determine the conditions under which having flagella is most advantageous for adhesion. These findings strongly indicate that, in addition to their role in swimming motility, flagella are involved in attachment and can furthermore act as structural elements, enabling bacteria to overcome unfavorable surface topographies. This work contributes insights for the future design of antifouling surfaces and for improved understanding of bacterial behavior in native, structured environments.

microbial adhesion | structured surfaces | bacterial appendages | surface texture | surface wetting

The attachment of bacteria to solid surfaces is the first step in the formation of biofilms—communities of sessile microbes surrounded by a polymeric matrix (1, 2). A growing appreciation of the ubiquity and importance of biofilms in medicine and industry has led to a proliferation of antiadhesion strategies that include chemical, biological, and physical approaches (3–12). Attempts to block biofilm formation must also take into account the rapid evolution of bacteria and their ability to resist many chemical assaults (13–17). By preventing adhesion in a manner that is nontoxic for the bacteria as well as for the application (e.g., medical implants), there is hope that we may reduce the costs associated with biofilm formation without imposing selective pressures for the development of antibiotic resistance. Physical strategies, particularly the use of rationally designed surface topographies, have gained attention recently as highly nonspecific methods for prevention of attachment without the use of antimicrobials (6, 8, 11, 18–20).

Understanding how bacteria interact with surfaces that have roughness on the micrometer and submicrometer length scales (i.e., comparable with the length scale of the bacteria themselves) is critical to the development of antiadhesive topographies. Such surfaces are also relevant for a deeper understanding of the native bacterial lifestyle, because most surfaces in nature are not atomically smooth. Indeed, the microvilli of the intestines are between 80 and 150 nm in diameter (21), creating considerable topographic constraints for enteric pathogens that might attempt to colonize the epithelium. Geometric considerations suggest that surfaces with roughness on the bacterial length scale provide less available surface area and fewer attachment points for rigid bacterial bodies than smooth surfaces (Fig. 1*A*). However, the simplistic view of bacteria as rigid rods or spheres ignores the presence of bacterial appendages, such as pili and flagella (Fig. 1*A*, *Right*).

Previous work has demonstrated that type I pili and flagella are required for biofilm formation by *Escherichia coli* (22). Flagella have been suggested to aid in overcoming surface repulsive forces and, possibly, to aid in spreading of cells along a surface. Additionally, exopolysaccharides and surface antigens help to develop biofilm morphology (23, 24). It is possible that such extracellular features also play important roles in allowing bacteria to adapt and adhere to bumpy surfaces. Using wild-type cells and deletions of several biofilm-associated genes, we herein examine the role of surface appendages on adhesion to patterned substrates and show that flagella in particular appear to aid in attachment to surfaces inaccessible to the cell body, by reaching into crevices and masking surface topography. By measuring adhesion to various surface patterns, we are able to better separate the adhesive role of flagella from their role in improving surface access via swimming motility and to suggest that flagella may provide an additional, structural function in biofilm formation.

Results

E. coli cells form biofilms on surfaces submerged in liquid (25). A relevant clinical example of this is catheter-associated urinary tract infections by uropathogenic *E. coli*. We asked whether micrometer-scale surface topography could reduce bacterial adhesion to submerged substrates. By introducing bumps separated by valleys smaller than a cell diameter, we hypothesized that there would be reduced surface area available to cells, and thus adhesion would be diminished compared with smooth surfaces (Fig. 1*A*). To choose an appropriate surface pattern, we first required an accurate measurement of cell diameter. Due to the inadequate resolution of light microscopy and the distortion associated with sample preparations for electron microscopy (EM), we chose to use atomic force microscopy (AFM) to measure the diameters of hydrated cells. Exponential phase *E. coli* (strain ZK2686) cells were probed with an AFM in liquid using contact mode. The measured cell diameters were 0.60 ± 0.10 μm ($n = 48$).

We designed and manufactured silicon wafers with a honeycomb pattern using photolithography. These wafers acted as molds to generate polydimethylsiloxane (PDMS) surfaces with an array of hexagonal features 2.7 μm in height and 3 μm in diameter, separated by 440-nm trenches (designated as "HEX" patterns; Fig. 1*B*).

Author contributions: R.S.F., R.K., and J.A. designed research; R.S.F. and H.V. performed research; P.K. and M.K. contributed new reagents/analytic tools; R.S.F., H.V., and J.A. analyzed data; and R.S.F., H.V., R.K., and J.A. wrote the paper.

The authors declare no conflict of interest.

This article is a PNAS Direct Submission.

Freely available online through the PNAS open access option.

[1]To whom correspondence should be addressed. E-mail: jaiz@seas.harvard.edu.

This article contains supporting information online at www.pnas.org/lookup/suppl/doi:10.1073/pnas.1219662110/-/DCSupplemental.

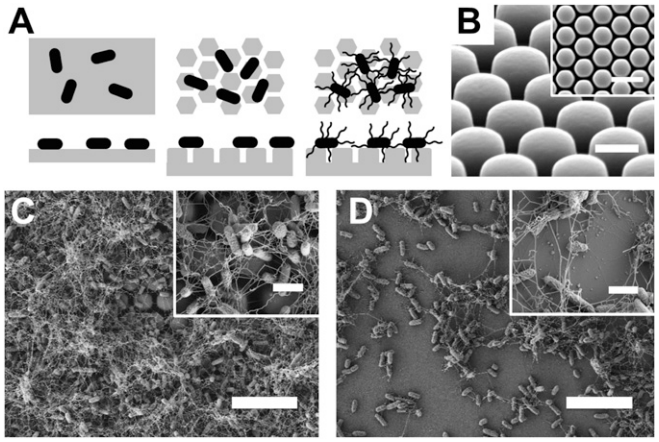

Fig. 1. Bacterial surface adhesion. (*A*) Schematics of *en face* (*Upper*) and cross-sectional (*Lower*) views of rod-like bacteria adhering to flat (*Left*) or patterned (*Center*) substrates and attachment of bacteria possessing surface appendages to a patterned substrate (*Right*), when the length scale of surface topography is on the order of the bacterial diameter. (*B*) Scanning EM of a HEX PDMS substrate. (Scale bar, 2 μm.) *Inset* is orthogonal view at lower magnification. (Scale bar: *Inset*, 5 μm.) (*C*) Scanning EM of wild-type *E. coli* grown for 24 h at 37 °C in M63+ on a HEX-patterned PDMS substrate. *Inset* is higher magnification. (*D*) *E. coli* grown on flat PDMS substrate. *Inset* is higher magnification. (Scale bars: in *C* and *D*, 10 μm; *Inset* in *C* and *D*, 2 μm.)

Notably, the spacing of the trenches was more than 1 SD below the measured mean cell diameter. We grew wild-type bacteria on smooth and HEX-patterned PDMS coupons submerged in M63+ medium. These static cultures were incubated for 24 h at 37 °C and then prepared for scanning electron microscope imaging (Fig. 1 *C* and *D*). Surprisingly, our observations indicated that there was more surface coverage by the *E. coli* cells on HEX than on flat surfaces. Furthermore, we noted the presence of a dense, fibrous network surrounding the surface-bound cells.

Matrix components are salient characteristics of most biofilms; indeed, many bacterial species, including *E. coli*, have been shown to produce several kinds of polysaccharide, protein, and DNA elements in their biofilm matrices. Because the *E. coli* cell bodies could not access the entire surface of HEX-patterned substrates, it seemed likely that the observed fibers were helping to augment surface attachment to these topographies. To identify the components of the fibrous material, we constructed and obtained mutants with deletions in known biofilm-associated genes, including the following: *wcaF*, coding for the polysaccharide colanic acid; *bcsA*, a cellulose gene; *fimA*, coding for type I pili; *csgA*, coding for curlin amyloid fiber subunits; and *flhD*, the master regulator for flagella synthesis. We grew each of these strains on HEX substrates as described above and imaged with a scanning EM (Fig. 2). All of the mutants resembled the wild type, except for Δ*flhD*, which had a clear lack of associated fibers. FlhD is a transcriptional regulator that controls expression of many genes including, but not limited to, the flagellar apparatus (26). To determine whether flagella or motility specifically were required for better colonization, we constructed deletion mutants for *fliC*, the flagellin subunit gene, and *motB*, a motor protein that enables flagellar rotation (Fig. 2). The Δ*fliC* mutant displayed the same phenotype as seen for Δ*flhD*, indicating that the observed effect was due to the absence of flagella. Furthermore, the Δ*motB* motility mutant was able to colonize the surface and it generated fibers similar to the wild type. These findings are consistent with the fibrous material being predominantly composed of flagellar filaments.

We examined the time course of adhesion for wild type and Δ*fliC* mutant on HEX-patterned versus flat surfaces to determine whether flagella play a role in the increased adhesion of the wild type to HEX surfaces observed in Fig. 1 *B* and *C*. To analyze this, we plotted the ratio of biomass on HEX/flat surfaces at different times over a period of 24 h. For both strains, there was a reduction in adhesion to the HEX surface versus the flat surface at 2 h, the earliest time analyzed (Fig. 3*A*). At later time points, however, the wild-type cells accumulated more on the HEX surfaces than on the flat surfaces. In contrast, the Δ*fliC* strain showed more biomass on flat surfaces than on HEX surfaces at all time points, although the ratio approached unity toward 24 h. These data suggest that, although adherence of wild-type cells appears to benefit from surface patterning, the cells lacking flagella are unable to exploit the additional surface area provided by the microtopography.

It had previously been shown that mutants lacking flagella (Δ*fliC*) or unable to rotate flagella (Δ*motB*) produce less robust biofilms than wild-type strains on flat surfaces (22). To determine whether this was also the case when cells are grown on patterned surfaces, we compared biofilm production of the wild type to that of the Δ*motB* and Δ*fliC* strains at 24 h. These strains were each grown on submerged flat and HEX-patterned PDMS coupons, as above, for 24 h, and adherent cells were fixed and quantified by acquiring confocal *z* stacks of hydrated cells. Consistent with previous findings (22), the Δ*motB* and Δ*fliC* strains each had significantly less biomass than the wild type regardless of surface topography (Fig. 3*B*). This indicates that motility, not just the presence of flagella per se, is required for optimal biofilm formation. Interestingly, although still more defective than wild type, the Δ*motB* mutant accumulated more biomass than Δ*fliC* on both

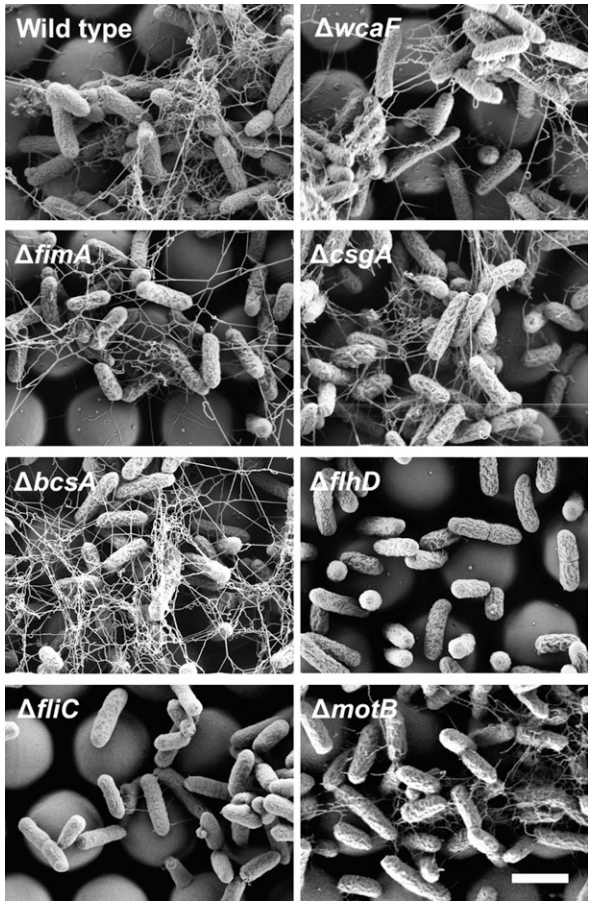

Fig. 2. Phenotypes of biofilm-associated knockouts on patterned PDMS. Wild-type (ZK2686) and mutant derivatives (as labeled) were grown on topographically patterned PDMS substrates for 24 or 48 h at 37 °C in M63+. Scanning electron micrographs depict the morphological properties of each strain. (Scale bar, 2 μm.)

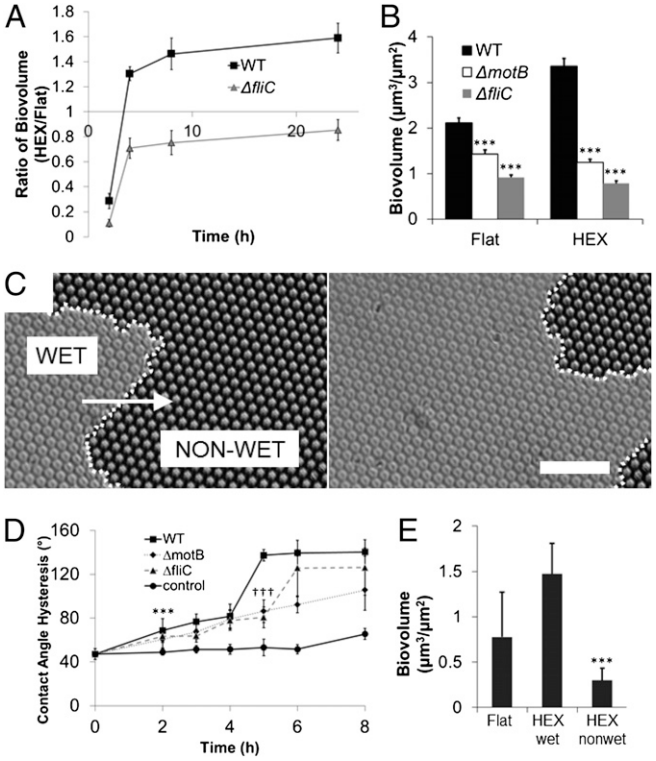

Fig. 3. Colonization of patterned substrates by wild-type and nonmotile bacteria and its relationship to surface wetting. (*A*) Biovolume on patterned (HEX) relative to flat substrates for wild-type and Δ*fliC* cells at various times. (*B*) Biovolume of cells adherent to submerged flat or HEX-patterned PDMS coupons after 24 h. Error bars indicate standard error of the mean of at least five independent experiments (five *z* stacks per experiment). ***$P < 0.001$ by Student's two-tailed *t* test, compared with WT. (*C*) Phase-contrast images of the advancement of the wetting front during culture, at 4 h. The meniscus (dotted line) advances through the patterned substrate, exposing channels between surface features, thus increasing available surface area for bacterial attachment. The area to the *Left* of the dotted line is fully wetted, whereas the area to the *Right* of the line contains air pockets. The white arrow indicates the direction of the wetting front progression. Thirty minutes have elapsed between the images on the *Left* and *Right*. (Scale bar, 20 μm.) For full movie, see Movie S1. (*D*) Contact angle hysteresis measurements of substrates that have been exposed to growing *E. coli* cells for increasing incubation periods or M63+ medium only, followed by sonication. Error bars represent SD. ***$P < 0.001$ by Student's two-tailed *t* test, comparing WT to control at 2 h. $^{\dagger\dagger\dagger}P < 0.001$ by Student's two-tailed *t* test, comparing WT to Δ*fliC* or Δ*motB*. See also Fig. S1. (*E*) Biovolume of cells adherent to submerged substrates after 2 h of culture. HEX substrates were either force-wet using ethanol followed by rinsing (HEX-wet), or left in their nonwetting state (HEX-nonwet). Error bars represent SD. ***$P < 0.001$ by Student's two-tailed *t* test, comparing HEX-wet to HEX-nonwet.

flat and patterned surfaces, suggesting that the presence of flagella, albeit paralyzed ones, may play a role in adhesion (Fig. 3*B*).

Although biofilm formation at 24 h was more robust in the wild type, both the flagella mutant and the wild type showed a dramatic preference for adherence to the flat substrate at the earliest (2 h) time point (Fig. 3*A*). Why was the patterned substrate successful at preventing adhesion at early time points, but not later? To better understand this phenomenon, we examined the substrates microscopically during the adhesion process. We noted that the HEX surface remained nonwetting, harboring trapped air bubbles within the trenches until ∼4 h, when the medium began to displace the entrapped air bubbles (Fig. 3*C* and Movie S1). This property, where the liquid phase rests atop a composite interface of air and solid, is termed the Cassie–Baxter wetting state, and is characteristic of superhydrophobic microtextured or nanotextured surfaces such as the lotus leaf (27, 28). We observed that this effect was lost over time in the presence of bacteria, resulting in complete wetting of the substrates (termed the Wenzel wetting state).

The difference in wetting properties of sterile medium versus medium with bacteria could be due to a change in surface tension of the medium or due to a change in surface energy of the substrate. Using the pendant drop method (29), we measured the surface tension of the M63+ medium to initially be 70.1 ± 0.6 mN/m at 20 °C. After 16 h of conditioning with *E. coli*, the medium was extracted by centrifugation and filtration, and its surface tension was measured to be 69.1 ± 0.5 mN/m at 20 °C. Although measurements were not carried out at culture temperatures, the predicted decrease in surface tension by increasing to 37 °C would be unlikely to cause wetting. Furthermore, conditioned medium did not cause wetting of fresh HEX substrates incubated at 37 °C.

To determine whether bacteria produce a substance that functions to precondition the surface and allow for increased wetting, we measured contact angle hysteresis (CAH) of water on dry HEX substrates after they had been placed in the presence of growing *E. coli* for 0–8 h (Fig. 3*D*). CAH is the difference between advancing and receding contact angles, and can be due to changes in surface energy or changes in surface topography. This value changes dramatically during Cassie–Baxter to Wenzel wetting transitions and so serves as a sensitive indicator of wetting state (30). All bacteria were removed by sonication before measurements, so as to avoid measuring properties of the bacteria themselves. CAH was significantly increased ($P < 0.001$) by 2 h of culture for all strains compared with control and continued to increase over the period measured. The medium-only controls did not wet during this period, resulting in the maintenance of a relatively low CAH. This difference in surface wetting properties indicates that the bacterial modification of the substrate surface energy (rather than modification of the liquid medium) is the dominant contributor to wetting properties. By 5 h, we observed a large increase in CAH for the wild type, but this was still significantly higher than CAH of the two mutant strains ($P < 0.001$). A commensurate increase did not happen until 6 or 8 h in the Δ*motB* and Δ*fliC* strains, indicating that the surface wetting brought about by bacteria–surface interactions is aided by the presence of motile flagella. Examining advancing and receding contact angles individually (Fig. S1), we observed that all samples maintained a relatively constant advancing contact angle over time with a slight downward trend, likely due to surface conditioning by bacteria. As the surface transitioned from the Cassie–Baxter to the Wenzel wetting state, there was an increase in drop pinning, which was measured as a decrease in the receding contact angle (30). It is this receding angle that changed more drastically and differentiated the behavior of the wild type from that of the mutant strains.

On flat substrates, the lack of microstructure prevents the possibility of a Cassie–Baxter wetting state; thus, the surface is entirely available to the cells from the outset. On the structured surfaces, wetting did not significantly occur until after 2 h. During this initial period, only the structure tips (not the trenches) are available to cells. Only upon wetting does the complete surface become available. We tested this by force-wetting the HEX substrates before inoculation with wild-type cells. At 2 h, we measured adherent biovolume, noting a significant increase in attachment to prewet surfaces compared with the untreated HEX substrates (Fig. 3*E*).

We reasoned that if the superior attachment by wild-type cells to HEX substrates is due to the access provided by their flagella, then varying feature size would only affect overall adhesion and biomass insofar as it changes overall surface area. In contrast, the Δ*fliC* cells would experience a reduction in attachment whenever portions of the substrate remained inaccessible to the cell body. We compared attachment of wild-type cells and Δ*fliC* mutants to substrates as we varied the feature diameters and spacings, maintaining a constant pitch (Fig. 4*A*). Indeed, the Δ*fliC* cells increased attachment as the feature spacing became larger, eventually surpassing their adhesion to flat substrates. For wild-type cells, the increased spacing had the opposite effect.

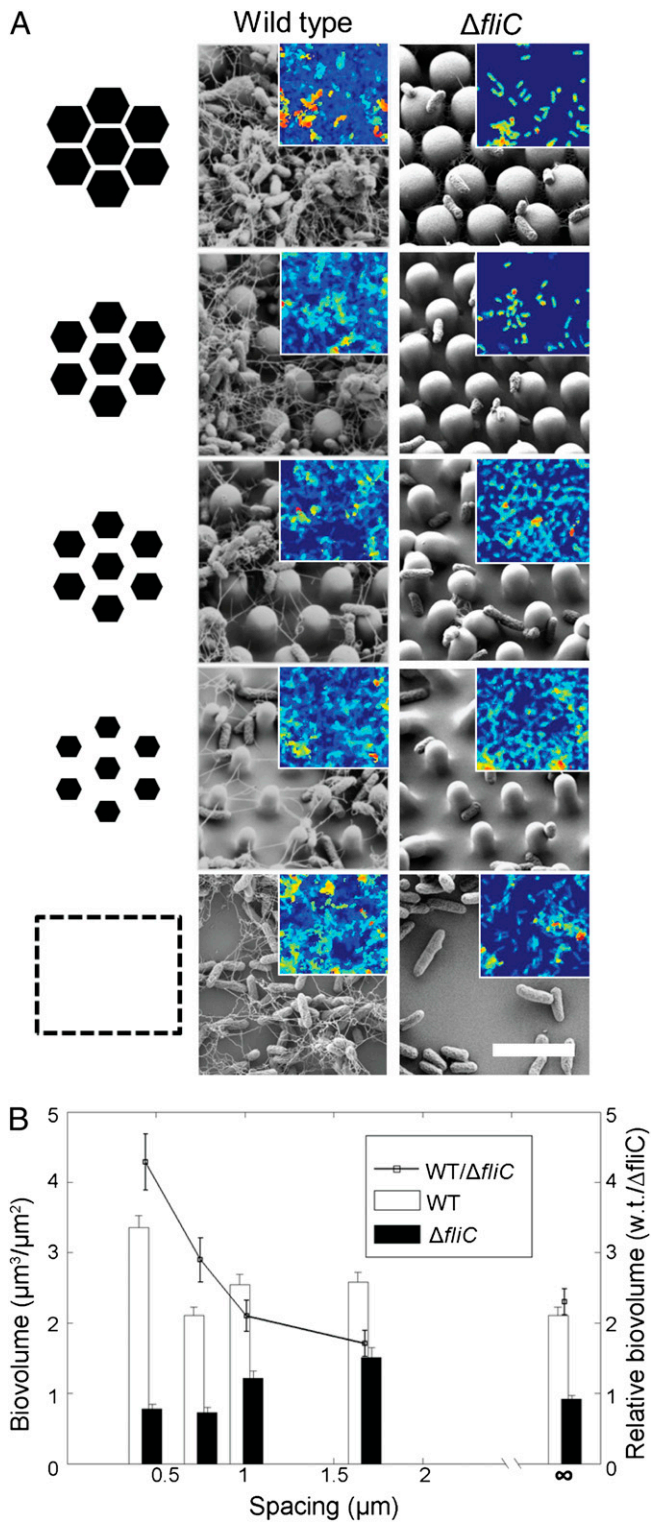

Fig. 4. Differential response of wild-type and Δ*fliC* cells to changes in surface feature spacing. (*A*) Schematic of underlying surface topography, illustrating increasing spacing with constant pitch (left column) and the scanning EM and confocal images of wild type and Δ*fliC* cells (center and right columns) grown for 24 h on corresponding PDMS substrates and then fixed. Samples were imaged in the hydrated state using confocal microscopy, and then dehydrated and imaged using scanning EM. Scanning EM images are shown, with representative thickness maps derived from confocal z stacks shown in the corresponding *Inset* (color mapping is for clarity and has arbitrary scale). (Scale bar, 5 μm.) (*B*) Biovolume was quantified for each topographical pattern and normalized to projected surface area. Biovolumes are shown for wild type and Δ*fliC* mutants (plotted as bars), as well as their ratios (black squares connected by lines). Error bars indicate SEM of ≥26 data points.

Whereas the wild-type cells had over four times the biomass of Δ*fliC* cells on HEX-patterned substrates (0.44-μm spacing), this difference was less than twofold on substrates with 1.70-μm spacing (Fig. 4*B*).

It appears that the benefit of having flagella is greater during adhesion to substrates with trenches smaller than the cell body than during adhesion to flat substrates or substrates with larger feature spacings. This phenomenon is unlikely to be due solely to the motility provided by flagella, because surface access should have been similar for all substrates tested. To further investigate the role of flagella in adhesion of wild-type cells to topographical substrates, we examined their dynamics in live cells during the adhesion process by fluorescently staining their flagellar filaments (31). Wild-type *E. coli* cells were placed in contact with HEX substrates and allowed to adhere. During the adhesion process, we observed attachment behavior. We noted that some cells were adhered by their flagella and exhibited tethering behavior (Fig. 5*A* and Movie S2). Additionally, some flagella inserted between surface features and attached within the submicron trenches, which was consistent with scanning EM findings, where flagella were observed to adhere between features (Fig. 5 *A* and *B*, and Movies S2 and S3). After 4 h of incubation, we observed alignment of some flagella with the underlying substrate. There was a tendency of flagella to orient along the planes of symmetry of the substrate (Fig. 5*C*), which implies that the filaments were interacting with the PDMS surface and responding to its topography.

Discussion

We herein set out to characterize the bacterial adhesive response to substrates with regular surface topography. Specifically, we were interested in the role of surface appendages in this response. We tested the hypothesis that surface feature length scale could, on its own, reduce bacterial attachment by reducing available surface area. Indeed, we observed that submicrometer trenches between features were able to reduce attachment of mutants without flagella. However, the geometric simplification of bacteria as rigid rods becomes invalid when applied to wild-type bacteria possessing surface appendages. Wild-type *E. coli* achieved better adhesion to surfaces with trenches than to flat surfaces. Because their surface appendages could access the trenches, the wild-type cells actually experienced an increase in available surface area on HEX substrates compared with flat, whereas the nonflagellated cells experienced the predicted decrease. These results indicate that bacterial adhesion to patterned surfaces is far more nuanced than anticipated by simplistic geometric models.

During the early adhesion process, we observed that all strains adhered more to flat substrates than to HEX substrates. Upon microscopic inspection, we could observe a wetting front progressing across the sample at 4–6 h into incubation, consistent with an initial Cassie–Baxter wetting state. Similarly, substrates removed from culture at 2 h appeared to be nonwetting, and the medium was observed to easily cascade off the substrates. At later time points, the samples remained wet upon removal. These observations were consistent with CAH measurements taken over 8 h of culture, showing a steady increase in hysteresis over time. Given this finding, it appears that, for short durations, the meniscus forming over each trench prevents bacterial adhesion and reduces surface availability to only the tips of the bumpy surface projections. At that time, structured surfaces do inhibit bacterial attachment. Δ*fliC* and Δ*motB* mutants were delayed in surface wetting of HEX substrates compared with the wild type, as measured by CAH. We conclude that motile flagella increase the probability of generating pinning points, thereby resulting in low receding contact angles. This difference in receding contact angle, but similarity in advancing angle between mutants and wild type indicates that their effects on surface chemistry are

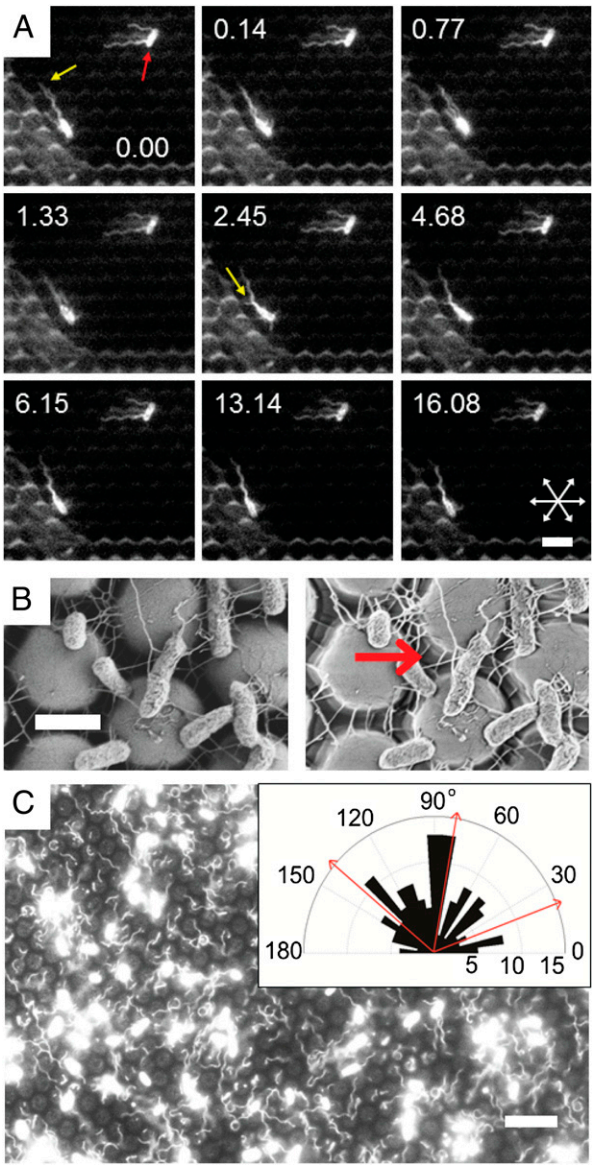

Fig. 5. Flagellar appendages "reach" and "grasp" to improve surface adhesion on patterned surfaces. (*A*) Selected frames from a video of Alexa 594-stained cells taken at 15 frames per second. Times are given (in seconds) in each panel. In frame 1, note that the upper cell (red arrow) is fully adherent (it remains stationary throughout the frames). Notably, its middle flagellum is nestled between the surface features slightly out of focus, because it is below the imaging plane. The other two flagella are resting atop the surface features in the focal plane. The lower bacterium is in the early steps of adhesion, tethered by one flagellum (yellow arrow), also nestled between the surface features. Its remaining free flagella continue to rotate rapidly until 2.45 s, at which time another (short) flagellum makes surface contact (yellow arrow). The cell body continues to slowly reorient as it makes more intimate contact (via other flagella and/or pili) and settles in its final position at 13.14 s. (Scale bar, 5 μm.) Axes of symmetry of the substrate are indicated by arrows in the bottom-right image. For full movie, see Movie S2. (*B*) Scanning EM images of the same field of wild-type *E. coli* grown on HEX PDMS posts. Images were acquired with Everhart-Thornley (*Left*) and in-lens detectors (*Right*). The difference in shadowing between the two images highlights the depth of penetration of the flagellar filaments into the channels between the surface features. Note specifically the region indicated by the red arrow. (Scale bar, 2 μm.) (*C*) Image of Alexa 594-stained cells after initial adhesion to HEX substrate. (Scale bar, 10 μm.) *Inset* shows angular histogram of filament orientations of adherent *E. coli*. The histogram illustrates preferential alignment of filaments along the two of the three planes of symmetry of the hexagonal surface pattern. Axes of symmetry of the substrate are indicated with red arrows.

similar, but they differ in their ability to expose surface features, which act as pinning points. We propose that the motor-driven motion of the flagella and/or cell body provides an input of vibrational energy that disrupts the metastable air–liquid interface and drives the recession of the liquid phase, thus enabling local wetting of trenches. This argument is further supported by microscopic observations of local advancement of the meniscus into trenches in areas where there is notable agitation by bacterial motion (Movies S4 and S5). Once the trenches are in contact with the culture medium, they can become conditioned with secreted proteins and/or medium components, and they become vacant attachment surfaces.

As has been noted in the literature, conditioning films can render surfaces more favorable for bacterial adhesion (32, 33). In our case, these conditioning films had the added effect of maintaining surface wetting. For the wild-type cells, accessibility of the interfeature trenches was critical in achieving increased adhesion. Once the initial layer of cells is able to anchor, these cells begin to alter the surface topography by their presence alone and can facilitate further attachment. In a sense, the adhesion of bacteria masks the surface features and acts as a topographical conditioning film, analogous to chemical conditioning films composed of macromolecules, which mask surface chemistry.

Several studies have reported that flagella are necessary for biofilm formation by *E. coli* and other bacteria such as *Listeria monocytogenes* and *Yersinia enterocolitica* (22, 34, 35). Furthermore, in addition to the presence of flagellar filaments, motor proteins that cause flagellar rotation are required. It has been suggested that swimming motility allows improved access to surfaces for initial attachment (22, 35). In low-shear environments, however, motility has been shown to have no effect on attachment of *E. coli* to glass (36). It has long been known that *E. coli* can adhere to surfaces via flagella (37), and somewhat more recently, several pathogenic strains have been shown to adhere to epithelial tissue using flagella-mediated adhesion (38–40).

Here, we found that the Δ*motB* mutant, which has flagella that are paralyzed, was only marginally better at adhering than the mutant lacking flagella and still had a marked reduction in surface adhesion compared with wild type (Fig. 3*B*). We posit that it is not simply the presence of flagellar filaments that enables access to the interfeature trenches, but the motion of these filaments as well. In examining the process of cell adhesion, it is apparent that the wild-type cells are able to rotate their flagella, even after initial attachment (Movies S2 and S3). This movement allows the flagella to explore the local geometry. There does not appear to be a strong long-range attractive force between the surface and the flagellar filament, but once the flagella adhere, it seems to be an irreversible process. From a functional standpoint, flagella should not typically be sticky, as this could impede swimming along a surface. Instead, there appears to be a low-affinity, high-avidity bond between flagella and the surfaces studied. This may be analogous to a cooperative binding event, where the initial binding reduces energy requirements for binding of additional monomers in the flagellar chain by forcing them into proximity with the surface. Still, there is some probability that nonmotile filaments would eventually make intimate contact with the substrate, perhaps aided by thermal motion. This possibility may account for the slight increase in biomass attained by Δ*motB* cells over Δ*fliC* cells, despite their ostensibly reduced translational diffusion, owing to the presence of flagella, which increase the effective hydrodynamic radius of the cells (41).

We have herein revealed that the flagella play an important role in surface adhesion, apart from their swimming function. This is supported by the finding that the surface-bound biomass of nonflagellated cells is less than 25% of the biomass of wild-type cells on HEX surfaces, but when interfeature spacing is large enough to accommodate the cell bodies, the Δ*fliC* cells achieve greater than 50% of the wild-type biomass. Our data indicate that the flagellar filaments, aided by motor-driven rotation, are able to penetrate subsurface features inaccessible to the cell bodies. Furthermore, they may bridge gaps between

features, thus weaving a web for improved attachment of additional cells. We speculate that the presence of multiple flagella in a peritrichous arrangement may be of substantial benefit for surface adhesion in topographical environments. In some species, such as *Aeromonas* spp. and *Vibrio parahaemolyticus*, lateral flagella are under differential genetic control from polar flagella (42). Efforts to isolate their individual functions have led to several interpretations concerning adhesion, virulence, and different forms of motility (43). We note that there are numerous enteric bacterial species possessing peritrichous and/or lateral flagella systems, which may be particularly important in an intestinal environment carpeted with microvilli.

Regardless of physiological interpretations, it is clear that bacterial adhesive abilities have evolved to enable attachment to a vast array of substrates. As the microscopic world tends to be highly structured, it is hardly surprising that bacteria should be able to cope with patterned landscapes. This work highlights the difficulties associated with prevention of bacterial surface colonization, and demonstrates the robustness and versatility of the bacterial adhesion repertoire. In light of this, we must incorporate multiple feature designs to improve antifouling surfaces. For example, if surfaces can be created that have stable Cassie–Baxter wetting states in biological settings, their superhydrophobicity may be exploited to reduce bacterial attachment, as we observed at early time points in the current study. The fact that bacteria can reach into small crevices and adhere with their flagella should prompt investigation into surfaces that can minimize flagellar adhesion, but can still be topographically controlled to limit access of the cell body and shorter appendages (such as pili). By increasing our understanding of the physiology of bacterial attachment in general and flagella–substrate interactions in particular, we can improve the parameters for the design of next-generation antibiofilm surfaces.

Materials and Methods

E. coli strain ZK2686 was used for all assays and as the genetic background for all deletion mutants. A summary of strains used is provided in Table S1. Growth and adhesion assays were carried out in static culture using M63 salts plus 0.5% (wt/vol) casamino acids and 0.2% (wt/vol) glucose (M63+). HEX substrates were cast in PDMS from a Bosch-etched silicon master, and feature sizes were varied using polypyrrole electrodeposition onto epoxy-negative replicas of the silicon master, followed by PDMS casting (44). Biovolume was quantified using image analysis of confocal *z* stacks. Detailed materials and methods are described in *SI Materials and Methods*.

ACKNOWLEDGMENTS. We thank Karen Fahrner for helpful discussions about flagella and bacterial swimming behavior, and Michael Bucaro and Wendong Wang for helpful experimental discussions. This work was partially funded by the Office of Naval Research under the award N00014-11-1-0641 and by the BASF Advanced Research Initiative at Harvard University. R.S.F. is supported by the National Science Foundation (NSF) Graduate Research Fellowship Program. Part of this work was carried out through the use of the Massachusetts Institute of Technology's Microsystems Technology Laboratories and the Center for Nanoscale Systems at Harvard University, a member of the National Nanotechnology Infrastructure Network, supported by the NSF under Award ECS-0335765.

1. Bos R, van der Mei HC, Busscher HJ (1999) Physico-chemistry of initial microbial adhesive interactions—its mechanisms and methods for study. *FEMS Microbiol Rev* 23(2): 179–230.
2. Costerton JW, Stewart PS, Greenberg EP (1999) Bacterial biofilms: A common cause of persistent infections. *Science* 284(5418):1318–1322.
3. Aslam S, Darouiche RO (2011) Role of antibiofilm-antimicrobial agents in controlling device-related infections. *Int J Artif Organs* 34(9):752–758.
4. Regev-Shoshani G, Ko M, Miller C, Av-Gay Y (2010) Slow release of nitric oxide from charged catheters and its effect on biofilm formation by *Escherichia coli*. *Antimicrob Agents Chemother* 54(1):273–279.
5. Park KD, et al. (1998) Bacterial adhesion on PEG modified polyurethane surfaces. *Biomaterials* 19(7–9):851–859.
6. Chung KK, et al. (2007) Impact of engineered surface microtopography on biofilm formation of *Staphylococcus aureus*. *Biointerphases* 2(2):89–94.
7. Carlson RP, Taffs R, Davison WM, Stewart PS (2008) Anti-biofilm properties of chitosan-coated surfaces. *J Biomater Sci Polym Ed* 19(8):1035–1046.
8. Xu L-C, Siedlecki CA (2012) Submicron-textured biomaterial surface reduces staphylococcal bacterial adhesion and biofilm formation. *Acta Biomater* 8(1):72–81.
9. Trautner BW, et al. (2012) Nanoscale surface modification favors benign biofilm formation and impedes adherence by pathogens. *Nanomedicine* 8(3):261–270.
10. Hachem R, et al. (2009) Novel antiseptic urinary catheters for prevention of urinary tract infections: Correlation of in vivo and in vitro test results. *Antimicrob Agents Chemother* 53(12):5145–5149.
11. Díaz C, Schilardi PL, Salvarezza RC, de Mele MFL (2007) Nano/microscale order affects the early stages of biofilm formation on metal surfaces. *Langmuir* 23(22):11206–11210.
12. Darouiche RO (2001) Device-associated infections: A macroproblem that starts with microadherence. *Clin Infect Dis* 33(9):1567–1572.
13. Francolini I, Donelli G (2010) Prevention and control of biofilm based-medical device related infections. *FEMS Immunol Med Microbiol* 59(3):227–238.
14. Davies D (2003) Understanding biofilm resistance to antibacterial agents. *Nat Rev Drug Discov* 2(2):114–122.
15. Stewart PS, Costerton JW (2001) Antibiotic resistance of bacteria in biofilms. *Lancet* 358(9276):135–138.
16. Mah TF, O'Toole GA (2001) Mechanisms of biofilm resistance to antimicrobial agents. *Trends Microbiol* 9(1):34–39.
17. Høiby N, Bjarnsholt T, Givskov M, Molin S, Ciofu O (2010) Antibiotic resistance of bacterial biofilms. *Int J Antimicrob Agents* 35(4):322–332.
18. Reddy ST, et al. (2011) Micropatterned surfaces for reducing the risk of catheter-associated urinary tract infection: An in vitro study on the effect of sharklet micropatterned surfaces to inhibit bacterial colonization and migration of uropathogenic *Escherichia coli*. *J Endourol* 25(9):1547–52.
19. Campoccia D, et al. (2006) Study of *Staphylococcus aureus* adhesion on a novel nanostructured surface by chemiluminometry. *Int J Artif Organs* 29(6):622–629.
20. Singh AV, et al. (2011) Quantitative characterization of the influence of the nanoscale morphology of nanostructured surfaces on bacterial adhesion and biofilm formation. *PLoS One* 6(9):e25029.
21. Brown AL, Jr. (1962) Microvilli of the human jejunal epithelial cell. *J Cell Biol* 12(3): 623–627.
22. Pratt LA, Kolter R (1998) Genetic analysis of *Escherichia coli* biofilm formation: Roles of flagella, motility, chemotaxis and type I pili. *Mol Microbiol* 30(2):285–293.
23. Danese PN, Pratt LA, Dove SL, Kolter R (2000) The outer membrane protein, antigen 43, mediates cell-to-cell interactions within *Escherichia coli* biofilms. *Mol Microbiol* 37(2):424–432.
24. Danese PN, Pratt LA, Kolter R (2000) Exopolysaccharide production is required for development of *Escherichia coli* K-12 biofilm architecture. *J Bacteriol* 182(12):3593–3596.
25. O'Toole GA, et al. (1999) Genetic approaches to study of biofilms. *Methods Enzymol* 310:91–109.
26. Liu X, Matsumura P (1994) The FlhD/FlhC complex, a transcriptional activator of the *Escherichia coli* flagellar class II operons. *J Bacteriol* 176(23):7345–7351.
27. Cassie ABD, Baxter S (1944) Wettability of porous surfaces. *Trans Faraday Soc* 40:546–551.
28. Barthlott W, Neinhuis C (1997) Purity of the sacred lotus, or escape from contamination in biological surfaces. *Planta* 202(1):1–8.
29. Stauffer CE (1965) The measurement of surface tension by the pendant drop technique. *J Phys Chem* 69(6):1933–1938.
30. Lafuma A, Quéré D (2003) Superhydrophobic states. *Nat Mater* 2(7):457–460.
31. Turner L, Ryu WS, Berg HC (2000) Real-time imaging of fluorescent flagellar filaments. *J Bacteriol* 182(10):2793–2801.
32. Murga R, Miller JM, Donlan RM (2001) Biofilm formation by gram-negative bacteria on central venous catheter connectors: Effect of conditioning films in a laboratory model. *J Clin Microbiol* 39(6):2294–2297.
33. Banerjee I, Pangule RC, Kane RS (2011) Antifouling coatings: Recent developments in the design of surfaces that prevent fouling by proteins, bacteria, and marine organisms. *Adv Mater* 23(6):690–718.
34. Duan Q, Zhou M, Zhu L, Zhu G (2013) Flagella and bacterial pathogenicity. *J Basic Microbiol* 53(1):1–8.
35. Lemon KP, Higgins DE, Kolter R (2007) Flagellar motility is critical for *Listeria monocytogenes* biofilm formation. *J Bacteriol* 189(12):4418–4424.
36. McClaine JW, Ford RM (2002) Characterizing the adhesion of motile and nonmotile *Escherichia coli* to a glass surface using a parallel-plate flow chamber. *Biotechnol Bioeng* 78(2):179–189.
37. Meadows PS (1971) The attachment of bacteria to solid surfaces. *Arch Mikrobiol* 75(4):374–381.
38. Yamamoto T, Fujita K, Yokota T (1990) Adherence characteristics to human small intestinal mucosa of *Escherichia coli* isolated from patients with diarrhea or urinary tract infections. *J Infect Dis* 162(4):896–908.
39. Erdem AL, Avelino F, Xicohtencatl-Cortes J, Girón JA (2007) Host protein binding and adhesive properties of H6 and H7 flagella of attaching and effacing *Escherichia coli*. *J Bacteriol* 189(20):7426–7435.
40. Girón JA, Torres AG, Freer E, Kaper JB (2002) The flagella of enteropathogenic *Escherichia coli* mediate adherence to epithelial cells. *Mol Microbiol* 44(2):361–379.
41. Tavaddod S, Charsooghi MA, Abdi F, Khalesifard HR, Golestanian R (2011) Probing passive diffusion of flagellated and deflagellated *Escherichia coli*. *Eur Phys J E Soft Matter* 34(2):1–7.
42. McCarter LL (2004) Dual flagellar systems enable motility under different circumstances. *J Mol Microbiol Biotechnol* 7(1–2):18–29.
43. Kirov SM (2003) Bacteria that express lateral flagella enable dissection of the multifunctional roles of flagella in pathogenesis. *FEMS Microbiol Lett* 224(2):151–159.
44. Kim P, et al. (2012) Structural transformation by electrodeposition on patterned substrates (STEPS): A new versatile nanofabrication method. *Nano Lett* 12(2):527–533.